Proc. Natl. Acad. Sci. USA
Vol. 76, No. 2, pp. 765–769, February 1979
Biophysics

Stability of lipid vesicles in tissues of the mouse: A γ-ray perturbed angular correlation study

(liposomes/drug-delivery system/γ-ray directional correlation)

MARCIA R. MAUK AND RONALD C. GAMBLE

Division of Chemistry and Chemical Engineering, Arthur Amos Noyes Laboratory of Chemical Physics, California Institute of Technology, Pasadena, California 91125

Communicated by John D. Baldeschwieler, November 13, 1978

ABSTRACT **The rate of phospholipid vesicle disruption in specific tissues of the mouse was followed by γ-ray perturbed angular correlation (PAC) spectroscopy. In these studies, high levels of ^{111}In–nitrilotriacetic acid complex are contained in unilamellar vesicles consisting of distearoyl phosphatidylcholine, cholesterol, and small amounts of other lipids which modify the surface properties. The PAC technique monitors the extent of vesicle breakup by measuring a time-integrated perturbation factor, $<G_{22}(\infty)>$. As the vesicles are broken open *in vivo*, the released $^{111}In^{3+}$ ions quickly bind to macromolecules and the $<G_{22}(\infty)>$ value decreases substantially. After administration of vesicles by various routes (intravenous, intraperitoneal, subcutaneous, and oral), the radioactivity and $<G_{22}(\infty)>$ values were determined for several tissues at intervals up to 24 hr. We conclude from these data that (*i*) the PAC technique in conjunction with standard γ counting methods provides unique information on the condition and location of vesicles in specific tissues, (*ii*) significant differences in vesicle integrity are found in various tissues, and (*iii*) both the means of administration and the presence of surface charge affect the vesicle stability and distribution. The carbohydrate analogues of cholesterol affect vesicle stability but not distribution.**

Extensive investigations have been conducted on the structure of liposomes and their interaction with mammalian cells, as summarized in several recent reviews (1–5). With the increasing interest in using liposomes as carriers of pharmacologically active agents, it becomes necessary to know not only the location of deposition of administered liposomes, but also the extent to which they remain intact. Recently, we have shown (6) that indium-111, encapsulated in liposomes, can be used to obtain this information. Conventional radioisotope tracer methods can determine the distribution of ^{111}In, and the overall structural integrity of liposomes can be monitored in live animals by γ-ray perturbed angular correlation (PAC) studies.

The PAC technique provides information on the tumbling rate of ^{111}In ions bound to ligands that possess different rotational correlation times (7–9). For example, $^{111}In^{3+}$ chelated to a small molecule and encapsulated in a liposome exhibits a fast tumbling rate. However, upon disruption of the bilayer, the $^{111}In^{3+}$ is released; it rapidly binds to a macromolecule in the surrounding solution and, consequently, shows a decreased tumbling rate (6). The chelator, nitrilotriacetic acid (NTA), is entrapped in the vesicles to minimize binding of indium cations to phospholipid headgroups. Thus, in a typical experiment in which NTA–$^{111}In^{3+}$ complex is entrapped in liposomes and injected into the bloodstream of a mouse, the PAC method can monitor the relative breakup of liposomes.

In earlier experiments (6), interpretation of data on the overall rate of vesicle destruction in live animals was limited by lack of information on structural integrity of vesicles in specific tissues. By using lipid vesicles that contain high levels of radioactivity (10), we are now able to obtain this information quickly. We examine here the effects of certain surface modifications and routes of administration on the stability of vesicles *in vivo*. The surface modifications are produced by incorporating various charged lipids and carbohydrate analogues of cholesterol into the lipid bilayer. In addition to intravenous injection, other means examined for introducing vesicles include oral, subcutaneous, and intraperitoneal administration.

MATERIALS AND METHODS

Materials. L-α-Dipalmitoyl phosphatidylcholine (Pal_2-PtdCho) (GIBCO, cont. no. C770259), L-α-distearoyl phosphatidylcholine (Ste_2-PtdCho) (Calbiochem, lot 740123), and cholesterol (Chol) (Sigma, lot 57C-7190) were used without further purification. Fucosyl and galactosyl analogues of cholesterol* (FucChol and GalChol, respectively) were gifts from Merck, Sharp & Dohme. Dicetyl phosphate (Cet_2-*P*) and stearylamine were purchased from Sigma, the trisodium salt of NTA from Aldrich, ultrapure $InCl_3$ from Ventron Corp. (Danvers, MA), and heat-inactivated calf serum from GIBCO. Cholesteryl [9,10-^{3}H]oleate, specific activity 11 Ci/g (410 GBq/g), was obtained from New England Nuclear. Carrier-free $^{111}InCl_3$ was purchased from Medi + Physics (Glendale, CA) and purified as described (6). The ionophore A23187 was a gift from Eli Lilly.

Preparation of Vesicles. Unilamellar vesicles with A23187 incorporated into the bilayer were prepared as described (10) by probe sonication of lipid mixtures in a buffer solution consisting of 1 mM NTA in phosphate-buffered saline (P_i/NaCl), which is 0.9% NaCl/5 mM sodium phosphate, pH 7.4. Vesicles of the following compositions were prepared: Pal_2-PtdCho:Chol:A23187 and Ste_2-PtdCho:Chol:A23187, both 2:1:0.004 (molar ratio); Ste_2-PtdCho:Chol:FucChol:A23187 and Ste_2-PtdCho:Chol:GalChol:A23187, both 2:0.5:0.5:0.004; and Ste_2-PtdCho:Chol:Cet_2-*P*:A23187 and Ste_2-PtdCho:Chol:stearylamine:A23187, both 7:2:1:0.01. Because all preparations contained A23187, reference to it will be omitted hereafter from the designated vesicle compositions. Tritiated cholesteryl oleate (1 μCi) was included in the mixtures as a marker for the lipid phase.

After sonication, annealing, and low-speed centrifugation

Abbreviations: PAC, γ-ray perturbed angular correlation; NTA, nitrilotriacetic acid; Pal_2-PtdCho and Ste_2-PtdCho, L-α-dipalmitoyl- and L-α-distearoyl phosphatidylcholine, respectively; Chol, cholesterol; FucChol and GalChol, fucosyl and galactosyl analogues, respectively, of cholesterol; Cet_2-*P*, dicetyl phosphate; P_i/NaCl, phosphate-buffered saline (0.9% NaCl/5 mM sodium phosphate, pH 7.4); $<G_{22}(\infty)>$, time-integrated perturbation factor.

* 6-(1-Thio-1-deoxy-β-L-fucopyranosyl)-1-(cholest-5-en-3β-yloxy)-hexane and 6-(1-thio-1-deoxy-β-D-galactopyranosyl)-1-(cholest-5-en-3β-yloxy)hexane.

The publication costs of this article were defrayed in part by page charge payment. This article must therefore be hereby marked "*advertisement*" in accordance with 18 U. S. C. §1734 solely to indicate this fact.

(10, 11), the NTA external to the liposomes was removed by passage of the preparation over a Sephadex G-50 column equilibrated with P_i/NaCl. Determination of the lipid concentration in the fractions was based on the tritiated cholesteryl oleate marker.

For several preparations, the vesicle-size distribution was determined by electron microscopy after negative staining with phosphotungstic acid.

Loading Procedure. The use of A23187 to facilitate loading of vesicles with $^{111}In^{3+}$ has been described (10). Briefly, after the Sephadex chromatography, vesicles with A23187 in the bilayer (typically 5 mg of lipid) were incubated at elevated temperatures (60°C for Pal_2-PtdCho, 80°C for Ste_2-PtdCho containing vesicles) for 30 min in P_i/NaCl containing 6.0 mM citrate (pH 7.4)/2.0×10^{-4} mM $InCl_3$ and $^{111}In^{3+}$, total volume 0.6 ml. Incubations were terminated by addition of 50 μl of 10 mM EDTA in P_i/NaCl. Nonloaded $^{111}In^{3+}$ was then removed by chromatographing the mixture on Sephadex G-50 equilibrated with P_i/NaCl. Approximately 90% of the added $^{111}In^{3+}$ was loaded, with specific activities of up to 300 μCi/mg of lipid.

Studies *In Vitro*. The effect of serum on the permeability of vesicles containing $^{111}In^{3+}$ was monitored by the PAC technique (6–9). These studies used a γ-ray coincidence spectrometer (7) to monitor changes in the rotational correlation time of the ^{111}In ion by measuring the time-integrated perturbation factor [$<G_{22}(\infty)>$] of solutions that contain $\approx$16 μCi of $^{111}In^{3+}$. Encapsulated $^{111}In^{3+}$ (existing at the NTA–$^{111}In^{3+}$ complex) exhibits a high $<G_{22}(\infty)>$ value due to its rapid tumbling. Disruption of the lipid bilayer causes release of the $^{111}In^{3+}$, which rapidly binds to serum proteins (6), resulting in a decrease in the rotational correlation time of the $^{111}In^{3+}$ as shown by a decrease in $<G_{22}(\infty)>$. When complete release of entrapped NTA–$^{111}In^{3+}$ was desired, the vesicles were disrupted by addition of isopropanol. All $<G_{22}(\infty)>$ values were measured at room temperature and were corrected to a standard sample size, 0.20 ml in a 10 × 75 mm glass tube.

Studies *In Vivo*. Vesicles containing $^{111}In^{3+}$ were administered to Swiss–Webster mice (18–22 g) orally or by intravenous (via tail vein), subcutaneous, or intraperitoneal injection. PAC studies on live animals required $\approx$16 μCi of $^{111}In^{3+}$ per mouse; administration of a minimum of 150 μCi of $^{111}In^{3+}$ per mouse was necessary for PAC studies on individual tissues. Radiolabeled vesicles were supplemented with unlabeled vesicles from the same preparation to adjust the total amount of administered lipid to the desired level. The volume administered orally was 75 μl; for injections, the volume was maintained at 0.40 ml/mouse by addition of P_i/NaCl when necessary.

PAC studies on live animals were conducted on mice confined within the barrel of a modified plastic syringe centered in the spectrometer, as described elsewhere (6, 12). The syringe was attached to a clock motor which allowed rotation of the mouse at 1 rpm to reduce artifacts arising as a result of inhomogeneous distribution of $^{111}In^{3+}$ within the animal. No other correctons of $<G_{22}(\infty)>$ values were made to account for the size or geometry of the mice.

PAC measurements on individual tissues were performed immediately after the animals were killed. At varying lengths of time after administration of $^{111}In^{3+}$, the mice were killed by cervical dislocation followed immediately by decapitation. Organs and tissues were washed with 0.9% NaCl, blotted, and weighed. PAC measurements of all tissues were completed within 1 hr. No change in $<G_{22}(\infty)>$ value was observed for samples remeasured within this time period. The distribution of injected radioactivity was determined by assaying the tissue samples in a well-type γ-ray spectrometer. Distributions are reported on a per organ basis. Blood was assumed to comprise 7.3% of the total weight of the animal.

RESULTS

Establishment of Standard Conditions. Measurement of $<G_{22}(\infty)>$ values for $^{111}In^{3+}$ provides an estimate of the rotational correlation time of the molecule to which the ^{111}In ion is bound (9). Values of $<G_{22}(\infty)>$ for $^{111}In^{3+}$ in various environments are shown in Table 1. NTA–$^{111}In^{3+}$ complex that is not encapsulated in vesicles interacts rapidly with serum and exhibits an accompanying decrease in $<G_{22}(\infty)>$ (6, 10). The slightly reduced values for the complex entrapped in vesicles presumably result from limited interaction of the $^{111}In^{3+}$ with the phospholipid headgroups or from some restriction of the rotational mobility of the complex when it is confined within the aqueous compartment of a vesicle. Electron microscopy indicates that the Ste_2-PtdCho:Chol vesicles are slightly larger than the Pal_2-PtdCho:Chol vesicles (mean diameters of 720 ± 40 Å and 650 ± 20 Å, respectively). No change in the mean diameter of the vesicle preparations could be detected when the carbohydrate analogues of cholesterol were substituted for part of the cholesterol in the bilayer.

The data in Table 1 show that both the Pal_2-PtdCho and Ste_2-PtdCho vesicle systems maintain their structural stability in the presence of serum at room temperature. However, at 37°C serum has a very marked adverse effect on the stability of Pal_2-PtdCho:Chol vesicles. In order to examine the role of vesicle bilayer and surface constituents on vesicle stability *in vivo*, it is imperative to select as a standard lipid system one which exhibits substantial stability *in vitro*. The Ste_2-PtdCho:Chol appears to satisfy this requirement, and for purposes of comparison it is used as the standard system throughout this investigation.

Preliminary experiments indicated substantial variability in the amount of radioactivity that was rapidly removed from the blood by the liver after administration of vesicles containing $^{111}In^{3+}$. For example, the amount of $^{111}In^{3+}$ recovered in the liver 3 hr after intravenous injection of Ste_2-PtdCho:Chol vesicles ranged between 18 and 80% of the injected dose. This variability is dependent on the amount of administered lipid (Fig. 1). To circumvent this dose-dependent and potentially unselective uptake of vesicles by the liver, administered dosages were standardized at 1.0 mg of lipid per mouse. Use of this amount, which is clearly sufficient to saturate the liver for the Ste_2-PtdCho:Chol system and presumably for the other systems

Table 1. $<G_{22}(\infty)>$ values for $^{111}In^{3+}$ in vesicles and various environments*

	Without serum	With serum	With serum, 30 min, 37°C	With serum + isopropanol
NTA–$^{111}In^{3+}$	0.70	0.19	0.19	0.18
Pal_2-PtdCho:Chol	0.59	0.54	0.43†	0.17
Ste_2-PtdCho:Chol	0.63	0.62	0.62‡	0.20
Ste_2-PtdCho:Chol: GalChol	0.60	0.60	0.61	0.24
Ste_2-PtdCho:Chol: FucChol	0.62	0.61	0.60	0.24
Ste_2-PtdCho:Chol: Cet_2-*P*	0.61	0.60	0.59	0.23
Ste_2-PtdCho:Chol: SA§	0.62	0.62	0.55	0.21

* All samples in P_i/NaCl prior to addition of 1 vol of heat-inactivated calf serum. Error in all measurements is ±0.02.
† 0.28 after 12 hr at 37°C.
‡ Value unchanged after 48 hr at 37°C.
§ SA, stearylamine.

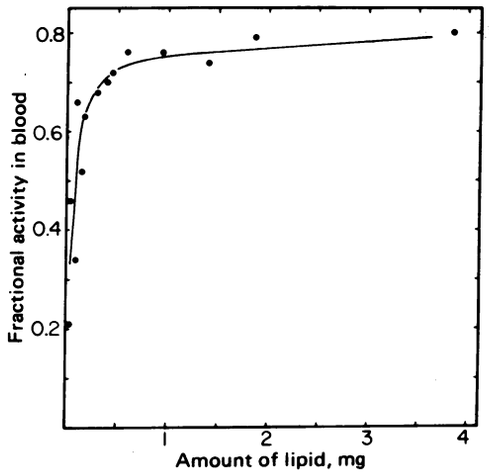

FIG. 1. Saturation of liver by lipid vesicles. Mice were killed 3 hr after receiving varying amounts of Ste_2-PtdCho:Chol vesicles by intravenous injection. Each 0.40-ml injection contained ≈3.0 μCi of encapsulated $^{111}In^{3+}$. The fractional activity in blood is defined as (total $^{111}In^{3+}$ in blood)/[(total $^{111}In^{3+}$ in blood) + (total $^{111}In^{3+}$ in liver)].

investigated, should also eliminate differences arising from minor variations in animal size.

Intravenous Administration. The tissue distribution of $^{111}In^{3+}$ was determined at various time intervals after intravenous administration of vesicles containing entrapped $^{111}In^{3+}$ (Fig. 2). The blood and liver contained most of the activity at short time points for all vesicle compositions examined. For example, with the Ste_2-PtdCho:Chol system 10 min after administration, 90 ± 14% and 11 ± 3% of the recovered activity were found in the blood and liver, respectively (average of four mice). For all distributions reported, no corrections were made for the blood content of the various tissues, which accounts for the greater than 100% activity noted at short times. At long time points, e.g., 24 hr (Fig. 2), the liver was the major site of deposition of $^{111}In^{3+}$ for all vesicle systems. However, negatively charged vesicles (Ste_2-PtdCho:Chol:Cet_2-*P*) showed significantly less, and positively charged vesicles (Ste_2-PtdCho:Chol:stearylamine) significantly more, $^{111}In^{3+}$ deposition in the liver than either the standard system or the vesicles containing the carbohydrate analogues. At all time points examined, the distribution of $^{111}In^{3+}$ after administration of free NTA–$^{111}In^{3+}$ complex did not resemble that from the vesicle systems. Recoveries for all systems were usually greater than 90% of the injected dose.

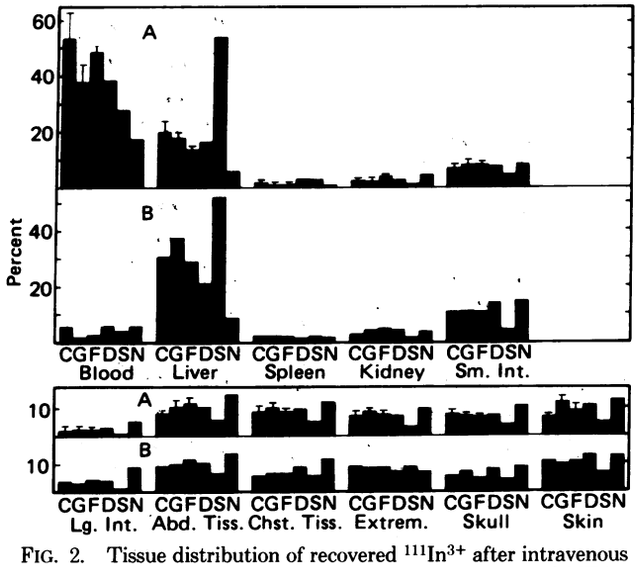

FIG. 2. Tissue distribution of recovered $^{111}In^{3+}$ after intravenous injection of NTA–$^{111}In^{3+}$ or vesicles containing entrapped NTA–$^{111}In^{3+}$. (*A* and *B*) Distributions for mice killed after 3 and 24 hr, respectively. C, Ste_2-PtdCho:Chol vesicles; G, Ste_2PtdCho:Chol:GalChol; F, Ste_2-PtdCho:Chol:FucChol; D, Ste_2-PtdCho:Chol:Cet_2-*P*; S, Ste_2-PtdCho:Chol:stearylamine; and N, free NTA–$^{111}In^{3+}$. Each bar represents the mean of two to six mice. Error bars for C, G, and F are ±SEM of six, four, and four mice, respectively. Because no corrections were made for the blood content of various tissues, the totals can be greater than 100% when significant radioactivity is in the blood. Each 0.40-ml injection contained 1.0 mg of lipid (no lipid in N) and ≥15 μCi of $^{111}In^{3+}$.

The overall stability of the vesicle preparations in live animals was examined by the PAC technique (Fig. 3). During the first 30 min after intravenous injection, only the negatively charged vesicles showed substantially reduced stability *in vivo*. At longer times it is clear that both charged vesicle systems, and to a lesser extent both carbohydrate analogue systems, show greater loss of structural integrity than the standard system.

The tissue distribution data at 3 hr (Fig. 2) shows similar profiles for the Ste_2-PtdCho:Chol and Ste_2-PtdCho:Chol:FucChol systems, with at most only a marginally lower $^{111}In^{3+}$ level in the liver for the Ste_2-PtdCho:Chol:FucChol system. Since the liver is presumably a site for destruction of vesicles, the distribution data do not explain the lower overall stability *in vivo* for the Ste_2-PtdCho:Chol:FucChol system (Fig. 3). However, examination of the $\langle G_{22}(\infty)\rangle$ values at 3 hr for individual tissues (Table 2) reveals that for several tissues (e.g., kidney, chest tissue, and skin) the extent of vesicle destruction is much greater with the Ste_2-PtdCho:Chol:FucChol system. With the charged vesicle systems the kidney and skin have even lower proportions of intact vesicles than observed with the Ste_2-PtdCho:Chol:FucChol system.

The blood content of the individual tissues will influence the observed $\langle G_{22}(\infty)\rangle$ value. This is a significant factor for highly vascular tissue such as the liver and at early time points when the $^{111}In^{3+}$ content of the blood is high. Within the limits of detection, all the $^{111}In^{3+}$ in the blood in the standard vesicle system remains encapsulated even at 24 hr after injection (Table 2). In contrast, the $\langle G_{22}(\infty)\rangle$ data for the Ste_2-PtdCho:Chol:Cet_2-*P* system suggest that some vesicle destruction occurs in the circulation. This destruction is seen in the lower $\langle G_{22}(\infty)\rangle$ values observed initially with the whole mice (Fig. 3).

Other Routes of Administration. The overall distribution and stability of the vesicle systems when administered by intraperitoneal injection approximates that observed after intravenous administration. However, considerable variability

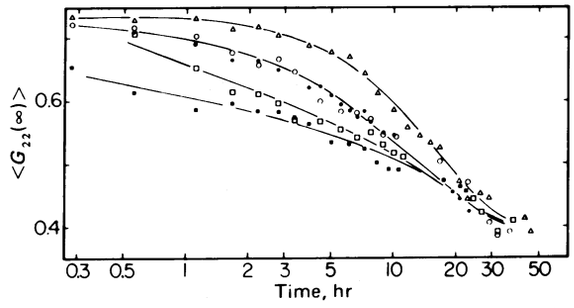

FIG. 3. Stability of vesicle preparations in live mice after intravenous administration. △, Ste_2-PtdCho:Chol vesicles; ○, Ste_2-PtdCho:Chol:FucChol; ●, Ste_2-PtdCho:Chol:GalChol; □, Ste_2-PtdCho:Chol:stearylamine; ■, Ste_2-PtdCho:Chol:Cet_2-*P*. Each set of points is the average of two mice. Each 0.40-ml injection contained 1.0 mg of lipid with 16 μCi of entrapped $^{111}In^{3+}$.

Table 2. $<G_{22}(\infty)>$ values of tissue after intravenous injection of vesicles containing $^{111}In^{3+}$ *

Tissue \ hr	Ste_2-PtdCho:Chol		Ste_2-PtdCho:Chol:FucChol			Ste_2-PtdCho: Chol:SA†	Ste_2-PtdCho: Chol:Cet_2-*P*
	3	24	3	12	24	12	12
Blood	0.62	0.61	0.61	0.57	‡	0.60	0.52
Liver	0.43	0.26	0.44	0.24	0.21	0.23	0.29
Spleen	0.54	0.24	‡	‡	0.25	0.17	0.28
Kidney	0.48	0.24	0.35	0.42	0.22	0.31	0.28
Sm. Int.	0.42	0.33	0.48	0.31	0.23	0.26	0.32
Lg. Int.	0.24	0.25	0.29	0.22	0.24	‡	‡
Abd. Tiss.	0.49	‡	0.45	0.37	0.29	0.25	0.28
Chest Tiss.	0.51	0.29	0.43	0.34	0.26	0.34	0.34
Extremities	‡	‡	0.41	0.26	0.22	‡	‡
Skull	0.49	0.25	0.42	0.32	0.19	‡	‡
Skin	0.50	0.28	0.37	0.35	0.30	0.27	0.27

* Variability between duplicate samples is ≤0.03.
† SA, stearylamine.
‡ Not measured.

in the rate and the extent of removal of vesicles from the injection site is observed with intraperitoneal administration.

After subcutaneous injection of radiolabeled vesicles, the $^{111}In^{3+}$ is recovered predominantly in the skin near the site of injection even 24 hr after administration (Table 3). A small amount of radioactivity is found in the chest tissue that is adjacent to the injection site. The $<G_{22}(\infty)>$ values on live mice (Fig. 4) clearly show that the vesicles remain intact for nearly 10 hr and then are rapidly degraded. For example, the $<G_{22}(\infty)>$ value for skin 12 hr after subcutaneous administration of Ste_2-PtdCho:Chol:GalChol vesicles was 0.40. Variation in the amount of vesicles administered subcutaneously (e.g., 0.1–1.5 mg of lipid and 0.1–0.42 ml total volume) did not cause any substantial difference in the vesicle lifetime.

In contrast to the subcutaneous results, orally administered unilamellar vesicles are destroyed within the time necessary to complete a single PAC measurement (Fig. 4). The tissue distribution of recovered $^{111}In^{3+}$ indicates that vesicles are not absorbed into the circulation from the gastrointestinal tract (compare low percentage in blood and liver). The $<G_{22}(\infty)>$ values for times corresponding to those in Table 3 show that the vesicles have broken open and the $^{111}In^{3+}$ has bound to the contents of the digestive system. For example, at 1 hr for the Ste_2-PtdCho:Chol system, the $<G_{22}(\infty)>$ values for the small and large intestine were 0.27 and 0.23, respectively. At 3 hr with the Ste_2-PtdCho:Chol:GalChol system, the $<G_{22}(\infty)>$ values for the stomach and small intestine were 0.27 and 0.25, respectively. The rate of vesicle destruction is not dependent on the amount of lipid administered orally over the range examined (0.1–1 mg). However, the rate of passage of radioactivity through the gastrointestinal tract is dependent on the feeding habits of the individual animals.

Table 3. Tissue distribution of recovered $^{111}In^{3+}$ *

Tissue \ hr	Subcutaneous injection		Oral administration	
	Ste_2-PtdCho: Chol:GalChol		Ste_2-PtdCho: Chol	Ste_2-PtdCho: Chol:GalChol
	12	24	1	3
Blood	1.0	0.3	0.04	0.05
Lung	0.1	0.05	0.02	†
Liver	1.1	2.2	0.02	0.01
Spleen	0.09	0.08	†	†
Kidney	0.4	0.4	0.02	0.01
Stomach	0.06	0.1	4.0	29
Small Int.	0.7	1.9	73	48
Large Int.	0.6	2.2	20	17
Abd. Tiss.	3.9	5.7	0.4	0.2
Chest Tiss.	22	14	0.1	0.7
Extremities	0.6	0.6	0.7	0.4
Skull	0.5	0.4	0.9	2.0
Skin	70	72	0.9	2.1

* Expressed as percent of total recovered radioactivity. For all systems, heart ≤0.04 and brain ≤0.01.
† Below limit of detection.

DISCUSSION

Entrapment of therapeutic materials in lipid vesicles can potentially afford protection for the material and direct it to desired locations. However, attempts to determine the fate of administered liposomes by classical radioisotope tracer methods have been complicated by the difficulty in distinguishing entrapped radioactivity from that released from the liposomes. We have recently shown (6) that PAC techniques can be used to establish the overall structural integrity of lipid vesicles in live animals by monitoring the molecular motion of $^{111}In^{3+}$ originally trapped in the aqueous phase of the liposomes. Using vesicles containing high specific activities of $^{111}In^{3+}$ (10), we are now able to determine the extent of vesicle destruction in individual organs and tissues, and, therefore, can more adequately interpret the overall rates of vesicle destruction observed in live animals.

Factors affecting the fate of lipid vesicles *in vivo* include the amount, composition, and route of administration of vesicles.

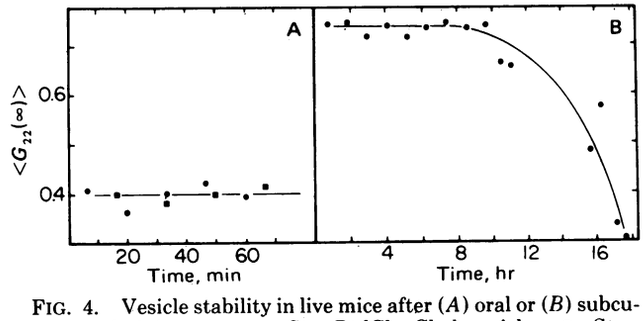

FIG. 4. Vesicle stability in live mice after (*A*) oral or (*B*) subcutaneous administration. ■, Ste_2-PtdCho:Chol vesicles; ●, Ste_2-PtdCho:Chol:GalChol. The data sets are the average of two mice.

Recently, Blumenthal *et al.* (13) described the presence of saturable sites on human lymphocytes for the transfer of liposomal contents into the cell interior. The presence of similar unselective saturable sites in the liver is suggested by recent work of Caride *et al.* (14) and Gregoriadis *et al.* (15). They found that administration of large quantities of nonradioactive liposomes (7 and 25 mg of lipid per mouse, respectively) resulted in a reduction in uptake of radiolabeled liposomes by the liver. By examining hepatic uptake as a function of administered dose, we show that <0.5 mg of our lipid vesicles is sufficient to saturate the liver of a mouse. Use of larger amounts of lipid should therefore overcome this rapid and unselective uptake by the liver and allow time for recognition of vesicle determinants by other tissues.

The possibility that surface carbohydrate groups may serve as determinants for recognition of liposomes by particular tissues is raised by the work of Lunney and Ashwell (16) which describes a specific hepatic receptor capable of recognizing and binding galactose-terminated glycoproteins. The results presented here show that the presence of either fucose or galactose on the surface of Ste_2-PtdCho:Chol vesicles causes no statistically significant alteration in the tissue distribution of the vesicles. These findings do not necessarily indicate the absence of appropriate receptors for the modified vesicles. Factors affecting conformation or accessibility may be important in recognition, as indicated in recent work by Bussian and Wriston (17) on the influence of cerebrosides on the interaction of liposomes with the HeLa cells. They incorporated synthetic cerebrosides containing glucose, galatcose, or lactose as the sugar component into multilamellar liposomes. The presence of galactose cerebroside caused a modest increase in uptake of liposomes by HeLa cells. However, they found that lactocerebroside had about a 2-fold greater effect on incorporation than galactocerebroside, suggesting that the glucosyl moiety of the disaccharide allowed better interaction of the terminal galactose with the putative cell-surface receptor.

Results presented here clearly indicate that the charge of the vesicles may be of great importance in achieving targeting of intact liposomes to desired tissues. The positively charged Ste_2-PtdCho:Chol:stearylamine vesicles were accumulated in the liver to a significantly higher level than any other system examined. The cause of this apparent targeting is not known, but it may arise from a change in the extent of interaction of vesicles with particular cell types or a change in the mechanism of liposome–cell interaction (1, 18). The decreased stability of charged vesicles observed for several tissues may also indicate a change in the mechanism of vesicle–cell interaction (e.g., from stable adsorption to endocytosis). The PAC measurements on individual tissues show that vesicle stability is also a function of tissue type. For example, vesicles in the blood can remain completely intact while those in other tissues, such as liver and intestine, are extensively disrupted.

The role of the route of administration on the fate of vesicles is most dramatic. Our findings with subcutaneous administration agree with a previous report (19) indicating that most of the vesicles remain at the site of injection. The PAC measurements indicate that the localized vesicles do remain intact for an extended period of time (≈10 hr). In contrast, we find that within 5 min after oral administration, the $^{111}In^{3+}$ entrapped in our vesicle systems becomes exposed to the contents of the stomach. Although a likely cause of this exposure is that the vesicles are disrupted, we cannot exclude the possibility that the release of indium results from an increase in the permeability of the bilayer in the gastrointestinal tract. No significant absorption of $^{111}In^{3+}$ from the gastrointestinal tract into the circulation was observed. However, in experiments on liposomally entrapped insulin, Patel and Ryman (20) conclude that in the stomach most of the insulin is still entrapped within liposomes 15 min after oral administration. This apparent discrepancy may arise from use of liposomes differing in composition and lamellar structure or from the method of analysis. Particularly, the chromatography used by Patel and Ryman may fail to distinguish between liposomally associated and entrapped insulin. This is a salient point in view of comments by Gregoriadis *et al.* (21) that insulin seems to interact with disrupted phosphatidylinositol liposomes, which may facilitate transport of insulin into the blood.

The techniques developed for examination of liposome stability by PAC techniques make possible the systematic examination of vesicle systems at both the tissue and live animal levels. It is anticipated that this type of information will be of considerable importance in developing optimal conditions for uptake and targeting of liposomally entrapped therapeutic agents.

We acknowledge the encouragement and support of Prof. John D. Baldeschwieler. We also thank Drs. T. Y. Shen and M. M. Ponpipom (Merck, Sharp & Dohme Research Laboratories) for helpful discussions during this work. This investigation was supported by grants from the National Institutes of Health (GM 21111-06), the National Science Foundation (CHE 75-15146-A03), and Merck Sharp & Dohme. This is contribution no. 5891 from the Arthur Amos Noyes Laboratory of Chemical Physics.

1. Pagano, R. E. & Weinstein, J. N. (1978) *Annu. Rev. Biophys. Bioeng.* **7**, 435–468.
2. Trouet, A. (1978) *Eur. J. Cancer* **14**, 105–111.
3. Fendler, J. H. & Romero, A. (1977) *Life Sci.* **20**, 1109–1120.
4. Gregoriadis, G. (1977) *Nature (London)* **265**, 407–411.
5. Poste, G., Papahadjopoulos, D. & Vail, W. J. (1976) in *Methods in Cell Biology*, ed. Prescott, D. M. (Academic, New York), Vol. 14, pp. 33–71.
6. Hwang, K. J. & Mauk, M. R. (1977) *Proc. Natl. Acad. Sci. USA* **74**, 4991–4995.
7. Meares, C. F., Sundberg, M. W. & Baldeschwieler, J. D. (1972) *Proc. Natl. Acad. Sci. USA* **69**, 3718–3722.
8. Leipert, T. K., Baldeschwieler, J. D. & Shirley, D. A. (1968) *Nature (London)* **220**, 907–909.
9. Meares, C. F. & Westmorland, D. G. (1971) *Cold Spring Harbor Symp. Quant. Biol.* **36**, 511–516.
10. Mauk, M. R. & Gamble, R. C. (1979) *Anal. Biochem.*, in press.
11. Lawaczeck, R., Kainosho, M. & Chan, S. I. (1976) *Biochim. Biophys. Acta* **443**, 313–330.
12. Goodwin, G. A., Meares, C. F. & Song, C. H. (1972) *Radiology* **105**, 669–702.
13. Blumenthal, R., Weinstein, J. N., Sharrow, S. D. & Henkart, P. (1977) *Proc. Natl. Acad. Sci. USA* **74**, 5603–5607.
14. Caride, V. J., Taylor, W., Cramer, J. A. & Gottschalk, A. (1976) *J. Nucl. Med.* **17**, 1067–1072.
15. Gregoriadis, G., Neerunjun, D. E. & Hunt, R. (1977) *Life Sci.* **21**, 357–370.
16. Lunney, J. & Ashwell, G. (1976) *Proc. Natl. Acad. Sci. USA* **73**, 341–343.
17. Bussian, R. W. & Wriston, J. C., Jr. (1977) *Biochim. Biophys. Acta* **471**, 336–340.
18. Poste, G. & Papahadjopoulos, D. (1976) *Proc. Natl. Acad. Sci. USA* **73**, 1603–1607.
19. McDougall, I. R., Dunnick, J. K., Goris, M. L. & Kriss, J. P. (1975) *J. Nucl. Med.* **16**, 488–491.
20. Patel, H. M. & Ryman, B. E. (1977) *Biochem. Soc. Trans.* **5**, 1739–1741.
21. Gregoriadis, G., Dapergolas, G. & Neerunjun, E. D. (1976) *Biochem. Soc. Trans.* **4**, 256–259.